

## Supplement of:

### Characterization of total OH reactivity in a rapeseed field: Results from the COV<sup>3</sup>ER experiment in April 2017

#### Supplementary material 1 : CRM characterization tests

In order to test the performance and the stability of the CRM/ PTR-MS system, several experiments were performed at the beginning, the middle and the end of the campaign. These tests also aimed to determine three correction factors, for the difference in humidity between C2 and C3, for OH recycling due to high NO mixing ratios and for the deviation from pseudo-first order kinetics.

- Correction for the difference in humidity between the C2 and the C3 levels

Experiments were performed by introducing a known amount of zero air at different humidity inside the reactor while the instrument is measuring C2. The dependency of the difference in the observed C2 on the difference of  $m/z$  37-to- $m/z$  19 ratio is investigated and used to correct the ambient C2 value. A linear least squares fit describes the dependency of C2 on the  $m/z$  37-to- $m/z$  19 ratio. The slope of the fit obtained from the experimental tests is then used to correct the C2 value during ambient measurements in the following way:  $C2_{corrected} = C2^* = C2 + p[(m/z37/m/z19)_{during\ C3} - (m/z37/m/z19)_{during\ C2}]$

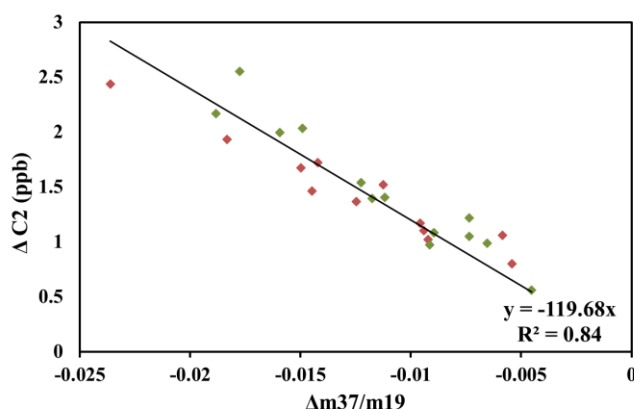


**Figure S1.a.** Linear least square fit of  $\Delta C2$  (ppbv) vs.  $\Delta(m37/m19)$  for the tests conducted on the field to assess the correction for humidity differences between C2 and C3. Green dots and red dots correspond to tests performed with ambient air and outgoing chamber air, respectively.

- Correction on C3 for the spurious OH production from the reaction between HO<sub>2</sub> (formed from H<sub>2</sub>O photolysis) and NO

To assess the required correction for C3 values, different amounts of NO were introduced inside the reactor while sampling humid zero air. The difference of measured C3 (ppbv) was plotted as function of NO concentration (ppbv).

$$C3_{corrected} = C3^* = C3_{measured} + \Delta C3$$

With  $\Delta C3 = a [NO]^2 + b[NO]$  as shown in figure S1.b.

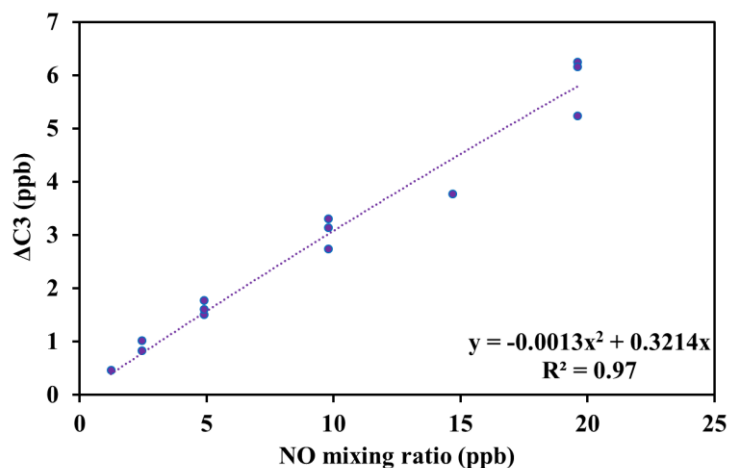


**Figure S1.b.** Experimental parameterization to correct for the NO interference, representing changes in C3 ( $\Delta C3$  ppb =  $C3_{\text{expected}} - C3_{\text{measured}}$ ) as function of NO mixing ratios (ppbv) in the reactor.

- Correction for not operating the CRM under pseudo-first-order conditions

Tests were performed by introducing different concentrations of two gas standards: propane with a relatively low reactivity with OH and isoprene which is relatively highly reactive with OH. Different pyrrole/OH ratios were investigated ranging between 1.7 and 2.7. As shown in figure S1.c, measured reactivity during tests was plotted against the expected one from calculation (calculated OH reactivity is the product of the gas standard concentration and its rate constant for the reaction with OH). The inverse of the resulting slopes represents the correction factors that vary for each compound, as function of the pyrrole/OH ratio.

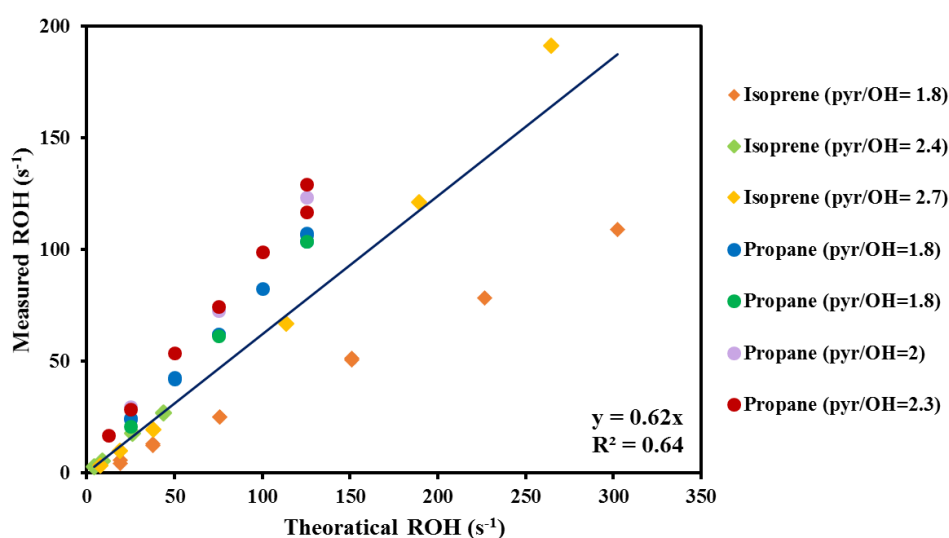


**Figure S1.c.** Measured ROH vs. the theoretical ROH for propane and isoprene, introduced at different concentrations and under different pyrrole/OH ratios. Circles and diamonds correspond to propane and isoprene tests, respectively.

Supplementary material 2 : CRM/PTR-MS samplig system

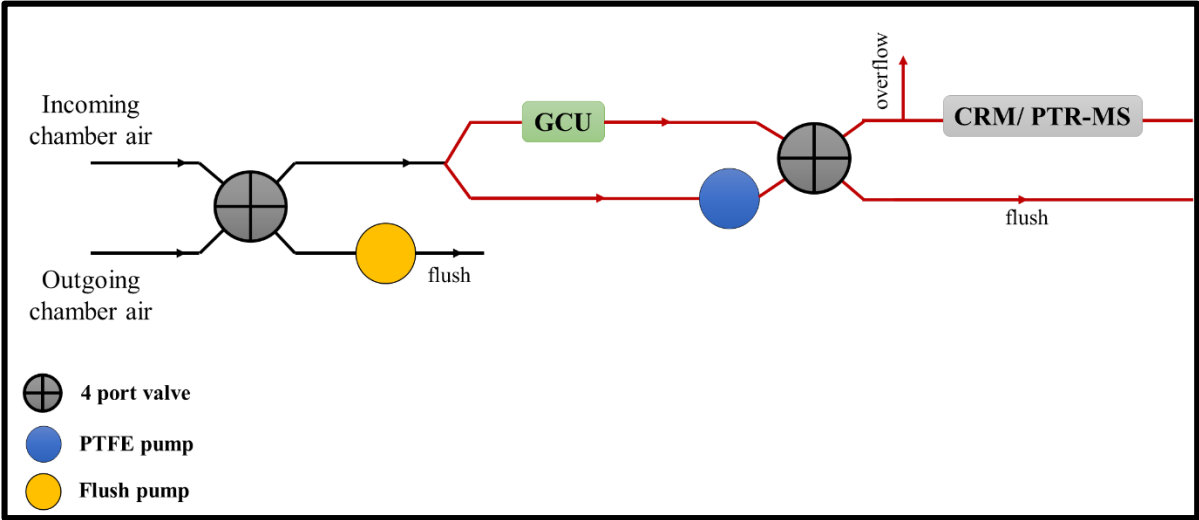


Figure S2. Schematic of the CRM/PTR-MS sampling system.

### Supplementary material 3: PTRQi-ToFMS VOCs mixing ratio computation

The pre-processing steps provided averages and standard deviations cps for the ion peaks selected  $R_i$ . The mixing ratio of the compound  $\chi_{i,ptr}$  (in ppbv) was calculated as in Abis et al., (2018) and Gonzaga Gomez et al. (2019):

$$\chi_{i,ptr} = 1.657 e^{-11} \times \frac{U_{drift} T_{drift}^2}{k p_{drift}^2} \times \left( \frac{cps_{R_i H^+}^{norm}}{cps_{H_3O^+}^{norm} + cps_{H_2O.H_3O^+}^{norm}} - \frac{cps_{R_i H^+}^{norm}(zeroair)}{cps_{H_3O^+}^{norm} + cps_{H_2O.H_3O^+}^{norm}(zeroair)} \right) \times S_i \quad (S3.1)$$

$$cps_{R_i H^+}^{norm} = \frac{TR_{H_3O^+}}{TR_{R_i H^+}} \times cps_{R_i H^+} \quad (S3.2)$$

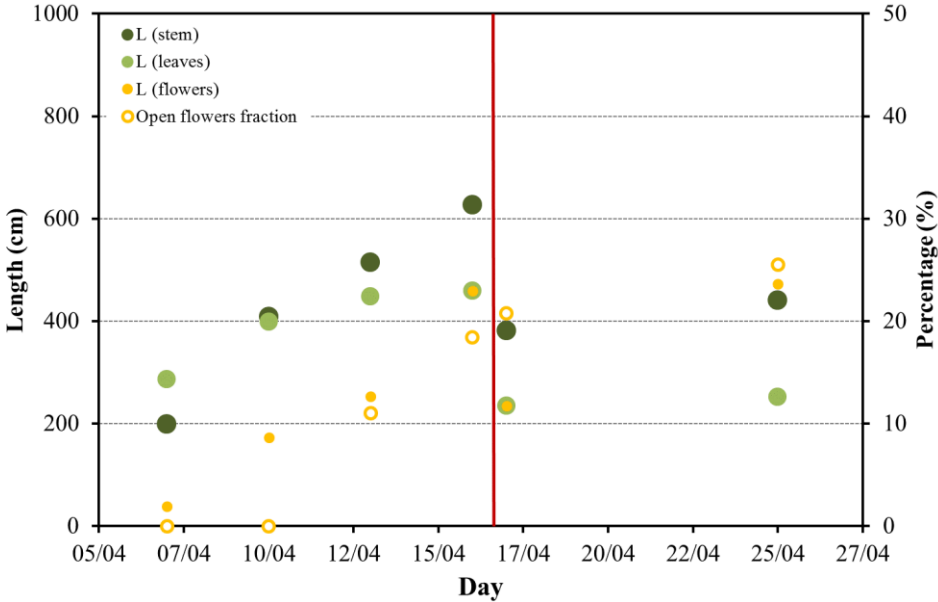
where  $U_{drift}$  is the voltage of the drift tube (V),  $T_{drift}$  is the drift tube temperature in Kelvin (K),  $cps_{R_i H^+}$  is the count per second (cps) of the product ion,  $cps_{H_3O^+}$  and  $cps_{H_2O.H_3O^+}$  are the cps of the source ion and the first water cluster,  $k$  is the protonation reaction rate assumed constant for all compounds ( $2.5 \cdot 10^{-9} \text{ cm}^3 \text{ s}^{-1}$ ), *norm* stands for normalized,  $TR_{H_3O^+}$  is the transmission factor for  $H_3O^+$ ,  $TR_{R_i H^+}$  is the transmission factor for mass of protonated compound  $R_i$ ,  $p_{drift}$  is the pressure in the drift tube, and  $S_i$  is the normalized sensitivity of the analyzer. Here *zeroair* stands for cps measured for zero air in the same conditions of pressure, temperature and voltage. The standard transmission curve from supplier was used to compute the normalized counts per seconds  $cps_{R_i H^+}^{norm}$  (Table S3).  $cps_{H_3O^+}^{norm}$  was computed from ion  $m/z$  21.022 ( $H_3^{18}O^+$ ) by multiplying by the isotopic factor 487.56, the first water cluster was taken as the ion peak  $m/z$  37.028. In equation (S3.1), the number  $1.657 e^{-11}$  is a constant specific to the instrument, accounting for the reaction time in the drift tube. The calibration procedures used to determine the zero and  $S_i$  are detailed in the manuscript.

**Table S3.** Standard Ionicon transmission curve used for computing the mixing ratio

$m/z$	TR	$\frac{TR_{H_3O^+}}{TR_{R_i H^+}}$
< 21	0.018	1.000
33	0.40	0.045
59	0.65	0.028
79	0.75	0.024
107	0.86	0.021
146	0.96	0.019
> 181	1.00	0.018

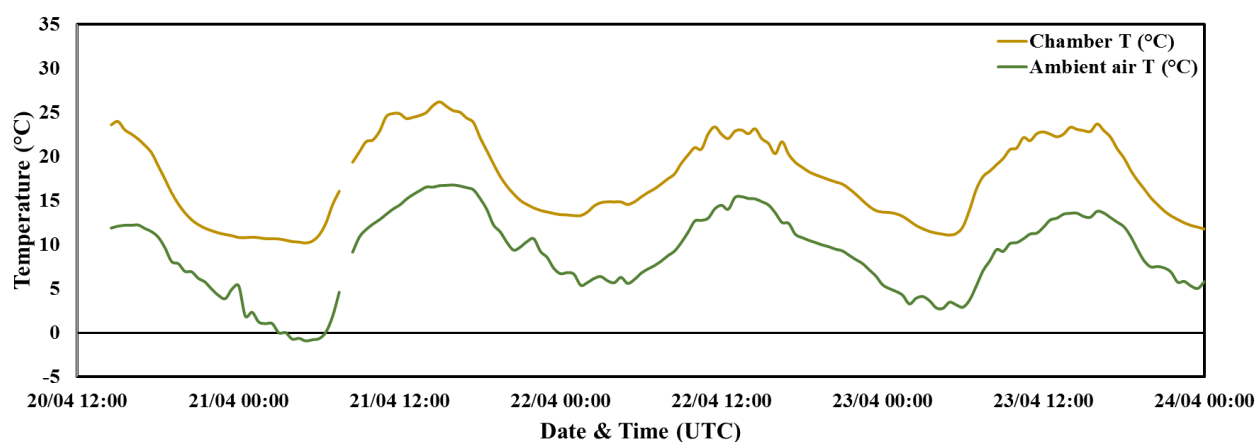
### Supplementary material 4: The rapeseed branch physiological evolution

At the beginning of our measurements (7<sup>th</sup> -15<sup>th</sup> of April), the rapeseed branch exhibited a rapid and more intensive growth, in terms of stem, leaves and flowers length as well as of number of open flowers, than during the last 10-day period (Figure S4), where the plant growth became more stable. Note that on the 15<sup>th</sup>, the chamber was uninstalled due to a planned fungicide application, and re-installed on the 17<sup>th</sup>, but on a higher part of the branch than before, including less stem, leaves and flowers.



**Figure S4.** Rapeseed branch evolution in the dynamic enclosure. The left vertical axis represents the length of the stem, total leaves and total flowers (in cm). The right vertical axis represents the percentage of open flowers. The red line indicates the day when the chamber was re-installed after the planned fungicide application.

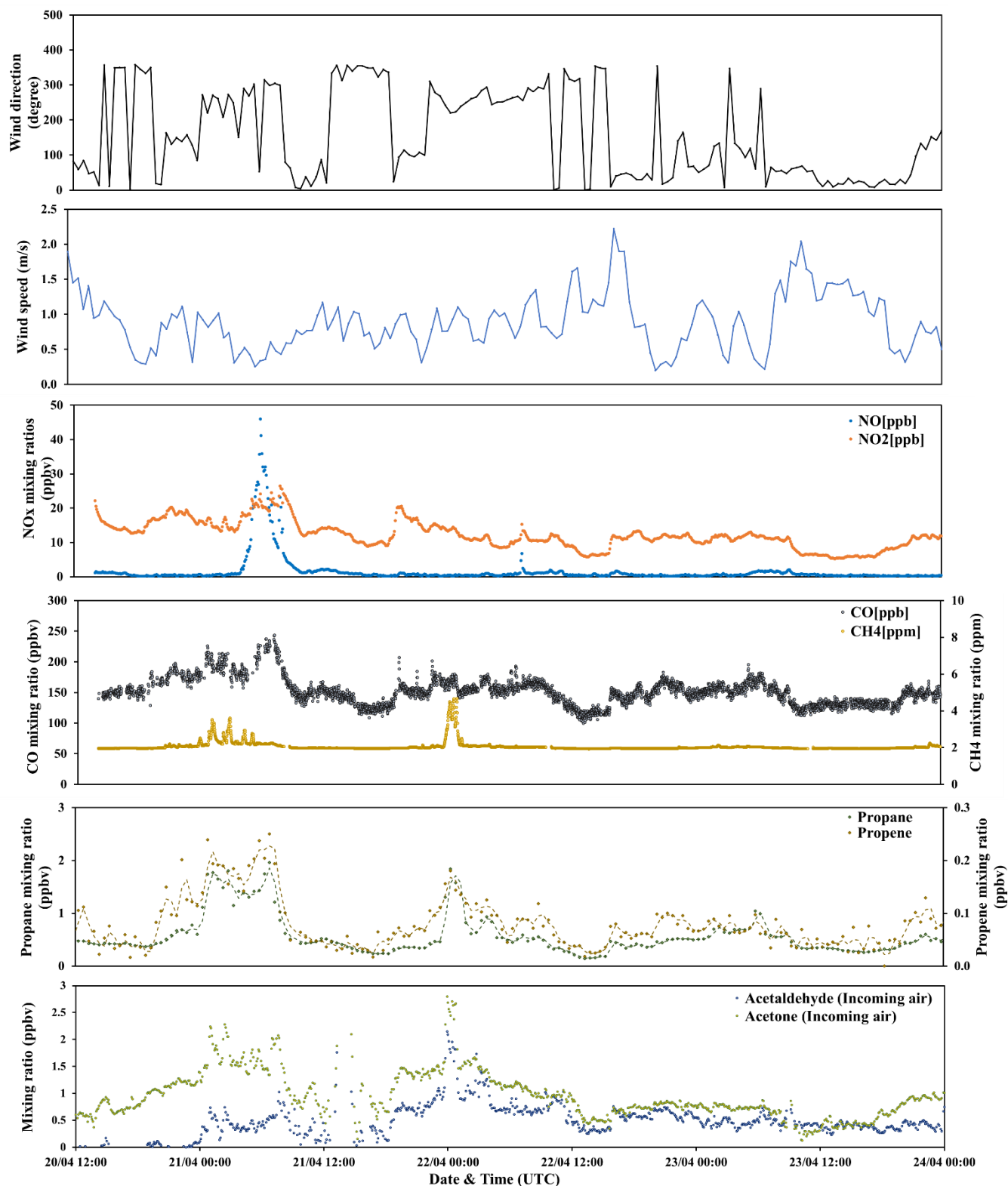
## Supplementary material 5: Comparison between temperatures recorded inside and outside the dynamic chamber



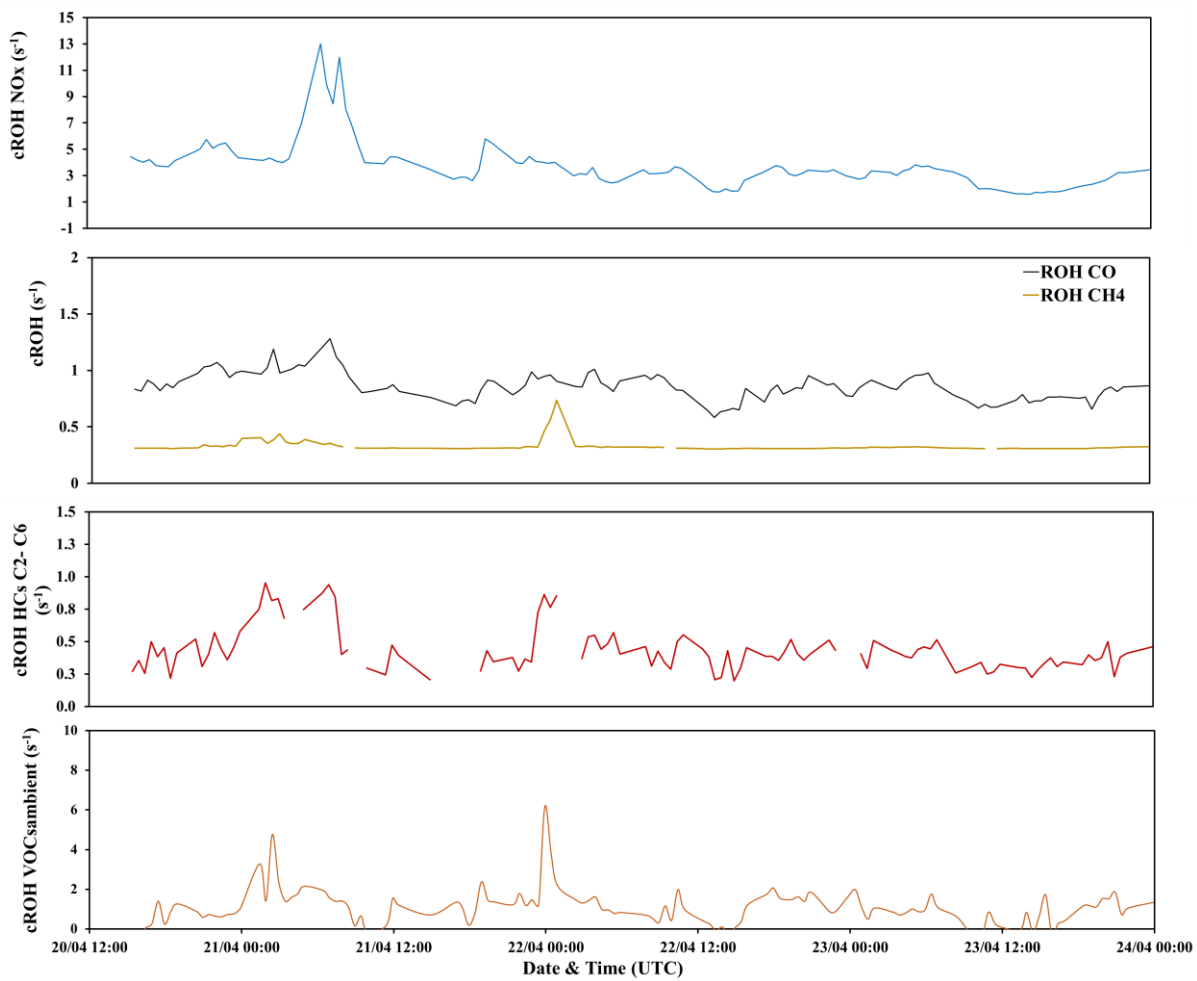
**Figure S5.** Temperature recorded inside the dynamic chamber (yellow) and in ambient air (green) during the measurement period between the 20th and the 23<sup>rd</sup> of April 2017.

Figure S5 shows the variability of temperatures recorded inside the chamber and in ambient air. Both temperatures had the same trend for the studied period, however a difference up to 12°C could be observed. This should be kept in mind when analyzing BVOCs and OH reactivity variability related to the enclosed rapeseed plant. Indeed, some BVOCs emissions are known to be temperature-dependent and their emissions could be enhanced under higher temperatures. However, higher concentrations of known/ detected BVOCs should result in higher  $mROH_{chamber}$ . Hence, these discrepancies in temperature should not affect the discussion on missing OH reactivity.

## Supplementary material 6: Anthropogenic VOCs and inorganic compounds in ambient air



**Figure S6.a.** Variability of NO<sub>x</sub> (NO, NO<sub>2</sub>), CO, CH<sub>4</sub>, propane, propene, acetaldehyde and acetone in ambient air, with wind direction and wind speed.



**Figure S6.b.** Variability of calculated OH reactivity of NO<sub>x</sub>, CO, CH<sub>4</sub>, total HCs C<sub>2</sub>-C<sub>6</sub> and total VOC<sub>Sambient</sub> (PTRQi-ToFMS).

## Supplementary material 7: Biogenic VOCs inside the chamber

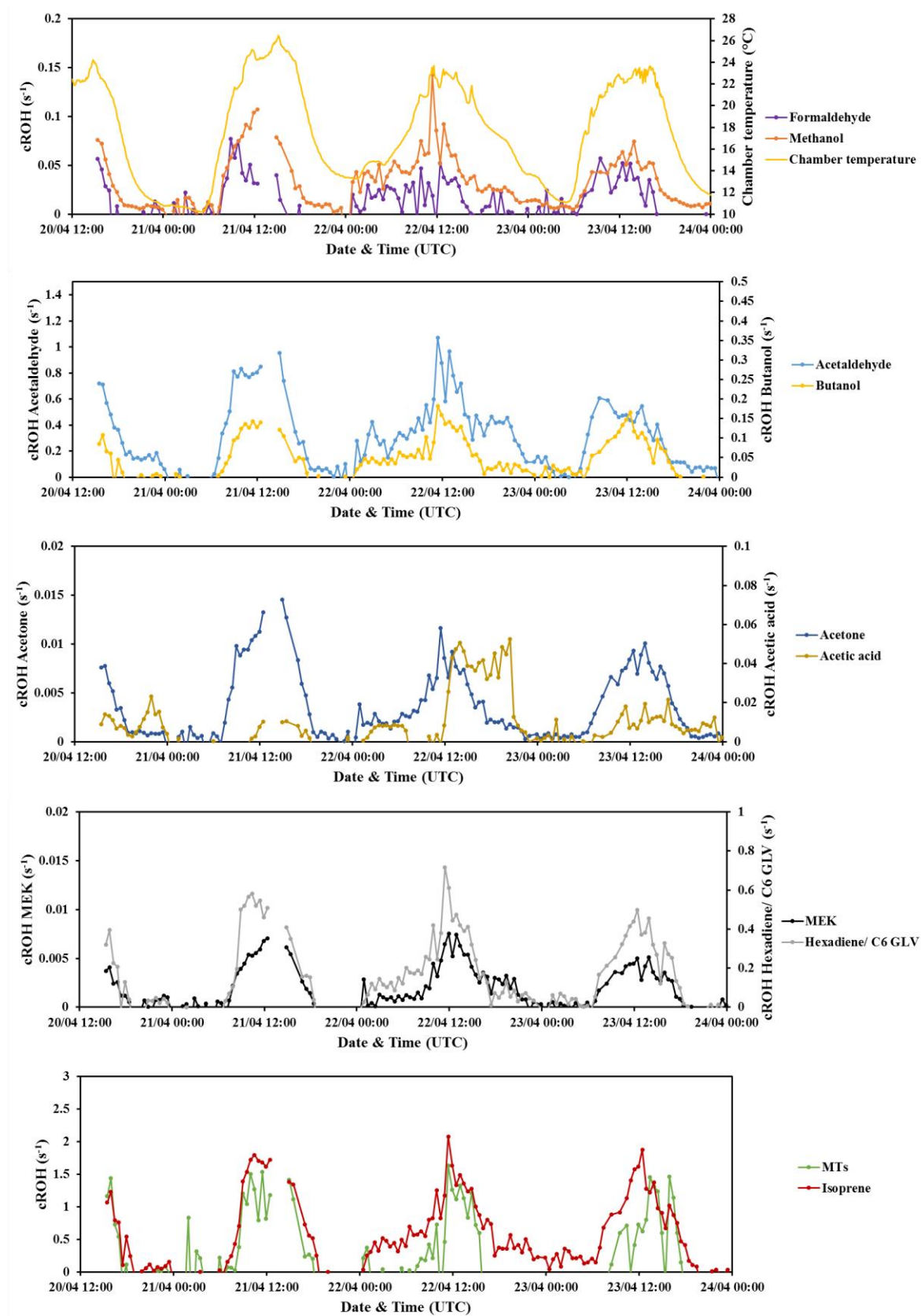


**Figure S7.** Variability of calculated OH reactivity of some biogenic VOCs emitted by the rapeseed plant ( $\text{VOCs}_{\text{rapeseed}} = \text{VOCs}_{\text{chamber}} - \text{VOCs}_{\text{ambient}}$ ).

## Supplementary material 8: Selection of PTRQI-ToFMS masses for missing OH reactivity investigation

**Table S8.** List of the 201 masses that correlate for 80 % and more with isoprene (m/z 69.070)

Protonated theoretical masses	R <sup>2</sup>
228.191, 248.981, 128.068, 180.101, 197.219, 72.017, 226.255, 376.073, 153.157, 196.212, 211.235, 264.264, 108.053, 86.059, 208.206, 87.078, 375.062, 229.198, 142.08	0.8
116.074, 158.088, 236.237, 98.026, 252.158, 102.086, 207.202, 134.068, 38.963, 185.13, 144.097, 85.027, 90.061, 183.206, 194.195, 170.191, 186.093, 85.064, 248.006, 184.207, 269.248, 210.226, 101.023	0.81
212.236, 159.131, 130.147, 303.291, 116.037, 169.189, 211.14, 250.25, 290.281, 209.217, 143.097, 172.096, 157.105, 193.187, 241.195, 154.166, 249.178, 182.196, 171.108, 255.218, 232.202, 205.082, 173.145, 204.175	0.82
88.048, 209.141, 278.282, 251.168, 54.938, 250.179, 133.098, 244.212, 161.096, 155.085, 141.09, 102.06, 155.175, 247.006, 235.227, 237.245, 187.076, 230.199, 263.263, 221.217, 243.213	0.83
234.221, 80.997, 127.076, 84.044, 174.147, 98.062, 60.048, 206.192, 287.258, 168.18, 87.042, 100.074, 181.19, 138.059, 289.265, 233.218, 205.186, 101.059, 141.159, 99.008, 142.163, 150.129	0.84
160.132, 262.244, 218.19, 148.116, 126.092, 260.238, 165.089, 187.155, 190.159, 57.033, 219.202, 192.176, 277.272, 137.058, 167.174, 231.202, 259.232	0.85
162.089, 180.18, 166.163, 70.039, 248.237, 128.148, 188.147, 246.22, 195.202, 138.133, 273.251, 245.219, 152.149, 201.171, 179.173	0.86
95.083, 146.119, 216.178, 106.037, 202.171, 165.158, 276.262, 217.183, 274.245, 191.172, 139.143, 215.181	0.87
261.247, 96.088, 275.254, 140.149, 247.23, 123.042, 176.142, 147.11, 189.15, 145.118	0.88
151.143, 117.087, 124.044	0.89
175.141, 39.023, 119.082, 100.117, 127.144, 105.032, 149.127, 123.115, 56.058, 56.024	0.90
68.052, 113.129, 44.055, 125.13, 124.117, 126.135, 178.161	0.91
82.074, 164.149, 109.1	0.93
110.103, 99.116, 72.088, 69.07, 177.157, 86.103, 112.119	0.94
163.142, 111.115, 58.068, 97.098, 98.104, 85.1	0.95
84.088	0.96
70.073	0.97

## Supplementary material 9: Sensitivity test on Isoprene's calculated OH reactivity

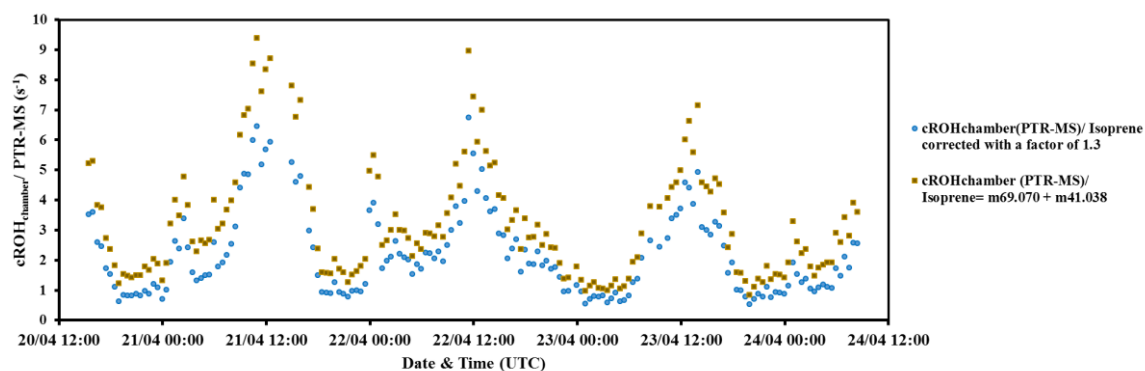


**Figure S9.** Variability of calculated OH reactivity using PTR-MS data with a correction of the isoprene signal ( $m/z$  69.070) by a factor of 1.3 (blue) and by summing the  $m/z$  69.070 with the potential fragment on  $m/z$  41.038 (yellow).

$m/z$  41.038 was identified as potential fragment of isoprene. In order to test the impact of taking this mass, or not, into account in OH reactivity calculation, this mass was accounted for by summing its mixing ratio with that of  $m/z$  69.070. An increase in OH reactivity was obtained with a maximum increase of  $3 \text{ s}^{-1}$ . This test explained  $1.3 \text{ s}^{-1}$  on average of day-time missing OH reactivity, meaning that the correction for potential fragmentation of isoprene would decrease the day-time missing OH reactivity by 20 % on average.